A New Generation of SIS Receivers for Millimeter-Wave Radio Astronomy

JOHN M. PAYNE, JAMES W. LAMB, JACKIE G. COCHRAN, AND NANCYJANE BAILEY, MEMBER, IEEE

A new generation of low-noise, dual-polarization heterodyne receivers covering all atmospheric windows between 68 and 300 GHz has been developed for the 12-m telescope on Kitt Peak, AZ, operated by the National Radio Astronomy Observatory (NRAO). A modular approach to the receiver construction has been used. Each receiver channel is constructed as a self-contained insert which is mounted in a dewar equipped with a closed-cycle 4 K refrigerator capable of cooling up to eight inserts, thereby enabling several frequency bands to be contained within one dewar. The telescope and receiver optics are so arranged that switching between frequency bands may be accomplished rapidly by rotating the optical elements placed in the signal path. Single-sideband noise temperatures ranging from 50 to 400 K are obtained across the frequency range.

I. Introduction

Receivers based on SIS (superconductor–insulator–superconductor) tunnel junction mixers are currently the most sensitive available for millimeter wavelengths and are replacing the cooled Schottky-diode mixer receivers that have been in use for many years.

SIS mixers use the sharp nonlinearity in the quasi-particle tunneling current between two superconductors separated by an oxide insulating layer. This is a single-electron tunneling process in contrast to the Josephson effect which results from the tunneling of superconducting Cooper pairs. The nonlinearity is so sharp that a quantum-mechanical description of the interaction with the incoming radiation is required [1], [2]. SIS mixers can exhibit nonclassical behavior such as conversion gain and negative input and output resistances. The great advantages of these mixers are very low intrinsic noise and a low local oscillator (LO) power requirement. One disadvantage is a requirement for a lower physical temperature than that required for Schottky mixers (around 4 K for SIS devices compared with 15 K for Schottky mixers). The mixers used in the receivers described here were developed by Kerr and Pan and have been fully described in the literature [3]–[6].

The signals detected in millimeter-wavelength radio astronomy are extremely weak, generally far smaller than the system noise and many hours of integration may be needed to achieve the required post-detection signal-to-noise ratio. Two independent receiver channels, sensitive to orthogonal polarizations, may be used. For unpolarized astronomical signals, this allows the two outputs to be combined after detection, to yield a factor of $\sqrt{2}$ improvement in sensitivity relative to one channel or a reduction in observing time of a factor of two to achieve the same signal-to-noise ratio.

A heterodyne receiver can be sensitive to two input frequency bands, the upper and lower sidebands, which are spaced on either side of the local oscillator frequency by the intermediate frequency (IF). Generally, the desired signal will appear in only one of these bands (known as the signal band). Single-sideband operation at millimeter wavelengths is particularly desirable as the objects studied by astronomers may have many spectral features that, in a system sensitive to both sidebands, can generate confusion due to contamination of the output by signals from the image sideband. Calibration of spectral line intensities is also simpler since relative gains at the signal and image frequencies (including atmospheric attenuation) need not be known as accurately. With the low-noise receivers now possible at millimeter wavelengths, the contribution to system noise from atmospheric noise and spillover radiation received in the unwanted sideband can be very significant. The unwanted band (the image band) is suppressed in some receiver systems, either by an external filter or by tuning the mixer to be narrow-band, so as to reject the image frequencies.

Several SIS heterodyne receivers have been described in the literature [7]–[14], but the receivers discussed here uniquely combine excellent sensitivity with full coverage of the atmospheric windows, optional double sideband or true single sideband (>20 dB image rejection) operation and dual polarization.

Manuscript received February 11, 1993; revised June 2, 1993. The National Radio Astronomy Observatory is operated by Associated Universities, Inc. under cooperative agreement with the National Science Foundation.

J. M. Payne, J. W. Lamb, and J. G. Cochran are with the National Radio Astronomy Observatory, Tucson, AZ 85721.

N. Bailey is with the National Radio Astronomy Observatory, Charlottesville, VA 22903.

IEEE Log Number 9400199.

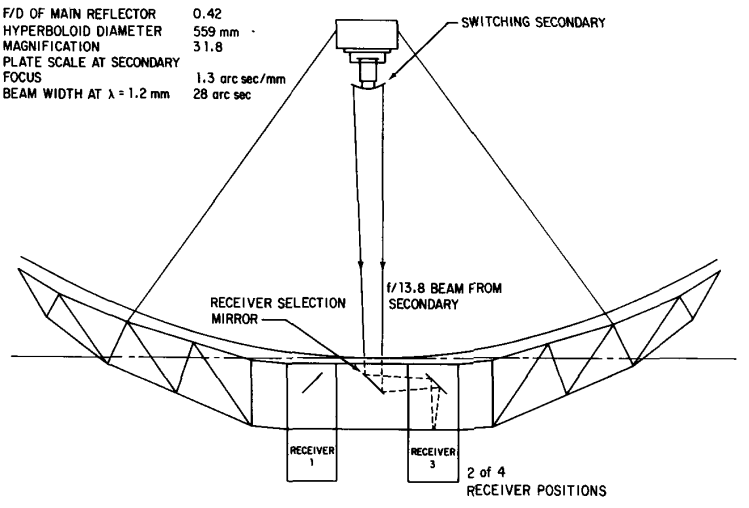

Fig. 1. The optical arrangement of the 12-m telescope.

Two receivers are described here, a low-frequency receiver (68–116 GHz, 130–170 GHz) and a high-frequency receiver (200–300 GHz), which cover the three atmospheric windows between 68 and 300 GHz. The low-frequency receiver uses selective tuning of the mixer to achieve single-sideband operation. The high-frequency receiver uses an external quasi-optical diplexer placed in the input beam to terminate the mixer in a cold load at the image frequency. In this way, sky noise and unwanted astronomical signals added to the IF output by the receiver response at the image frequency are minimized.

A fuller description of the fundamentals of both millimeter-wave receivers and millimeter-wave astronomy is given in [15].

II. Installation of Receivers

The receivers are mounted on the telescope as shown in Fig. 1. Placing the receivers at the secondary focus has the following advantages over prime focus operation:

1) Several receivers covering different frequency ranges may be mounted on the telescope. Any receiver may then be selected by rotating the central mirror as shown in Fig. 1.
2) Beam switching may be accomplished at all frequencies by moving the subreflector [16].
3) The greatly increased depth of focus permits the use of quasi-optical devices to perform the polarization diplexing and image termination.
4) The secondary focus configuration results in lower system temperatures since spillover from the receiver intercepts the cold sky temperature rather than the warm ground.

This last point is particularly important for the very-low-noise receivers described here. The support structure around the subreflector may be seen as a lossy room-temperature load or may allow ground radiation to be reflected into the feed. A carefully designed smooth reflecting shield around the subreflector designed to direct the spillover to the main reflector can result in significant reduction in system temperatures. Such a shield has been installed on the 12-m telescope and has resulted in a reduction in system temperature of around 50 K at 230 GHz [17].

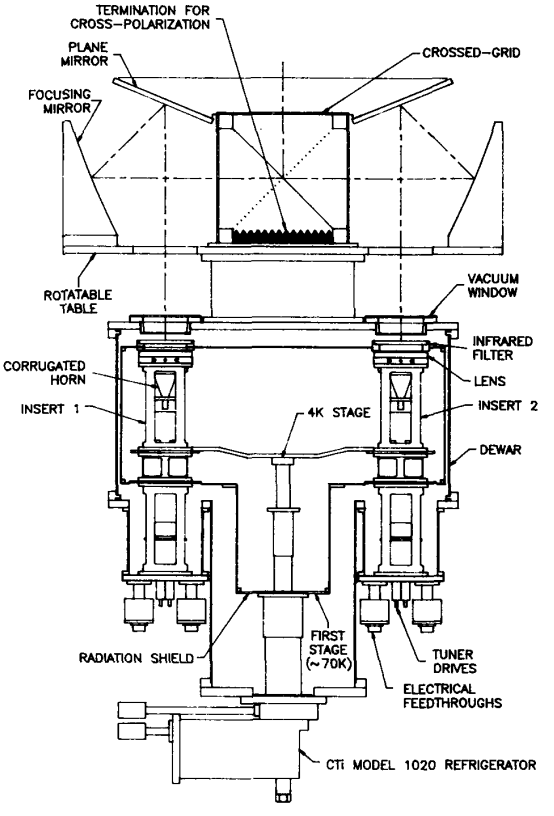

Fig. 2. Layout of the low-frequency receiver.

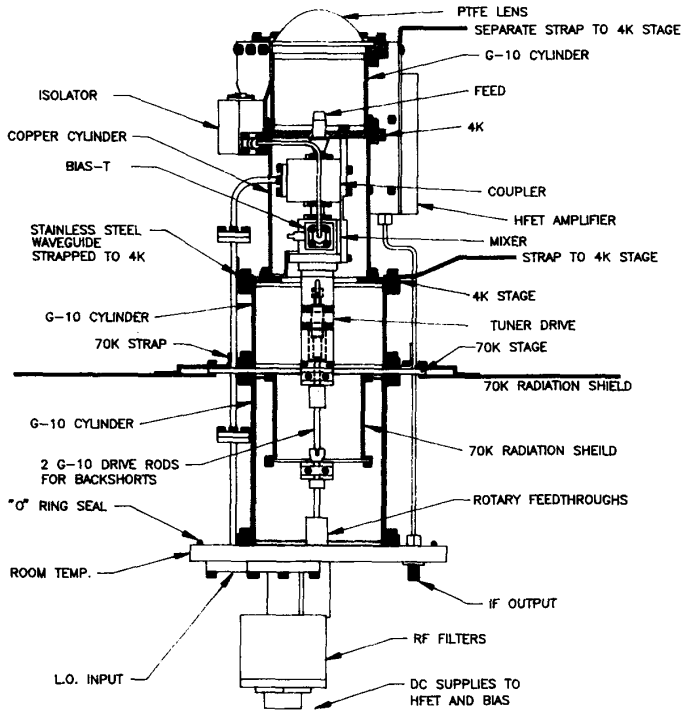

Fig. 3. High-frequency insert.

III. General Layout of Receivers

The high-frequency receiver (200–300 GHz) and the low-frequency receiver (68–116 GHz, 130–170 GHz) follow the same general layout as shown in Fig. 2, a diagram of the low-frequency receiver. A stainless-steel dewar 600 mm in diameter is used to house up to eight receiver inserts mounted on a circle 420 mm in diameter. A centrally located, closed-cycle, 4 K refrigerator is connected to the inserts via high-conductivity copper heat straps.

An optical assembly is mounted above the dewar and rotates about the central vertical axis. The outputs from the optical assembly are the two orthogonally polarized components of the input signal from the subreflector. These two signals pass into the two selected receiver inserts via vacuum windows and infrared filters cooled to an intermediate temperature.

Selection of any pair of inserts lying on a given diameter of the dewar may be made by rotating the optical assembly.

IV. Insert Design

The cooled receiver electronics for a polarization channel are contained within an insert which may be removed completely from the dewar as a unit. This allows for quick replacement and easy evaluation of the insert in a test dewar prior to installation in the main dewar. Figure 3 shows the construction of the high-frequency insert. A tower structure is used with stages at room temperature, ~70 K and 4 K. The stages are separated using thermally insulating G-10 fiberglass/epoxy cylinders.

At the top of the insert is a lens which focuses the incoming radiation into a corrugated feed horn. The horn is connected to a 20-dB branch-line coupler which combines the signal with the LO power. The output of the coupler feeds into the mixer mounted below it. A bias-T at the side of the mixer provides dc bias to the mixer through a four-wire supply and couples the IF out through an isolator to an L-band HFET amplifier [18] with a center frequency of 1.5 GHz and a bandwidth of 600 MHz. These components are all maintained at a temperature of 4 K, but the lens, isolator, and amplifier are separated from the mixer by a fiberglass/epoxy insulator and separate straps are taken directly to the 4 K refrigerator so that heat dissipated by the HFET and infrared radiation absorbed by the lens do not raise the mixer temperature through the thermal resistance in common straps and joints.

Local oscillator power is supplied to the coupler via stainless-steel waveguide which is internally plated with a 1-μm thickness of copper. This reduces the loss at the LO frequency without significantly sacrificing the thermal isolation of the stainless steel. In the case of the 200–300-GHz inserts, oversized waveguide[1] is used to further reduce the loss and to permit plating, while for the other inserts single-mode guide is used. The waveguide is heat sunk to the first stage and to the 4 K station. Stainless-steel coaxial cable is used for the IF output and it is also thermally strapped to those stages.

[1] For the 200–260-GHz receiver, WR-10 is used. For the 260–300-GHz receiver, WR-7 is used.

Each mixer has two remotely adjustable waveguide tuners with the exception of the 230–300-GHz mixer which is fixed-tuned. In the case of the low-frequency mixers, the tuning may be adjusted to give >20 dB rejection at the image frequency. For the high-frequency mixers, the image rejection is achieved optically as described later.

Each tuner is moved by means of a micrometer coupled by a 3-mm-diameter G-10 rod to a rotary vacuum feedthrough. The rod is thermally coupled to both the 70 and 4 K stages. A dc motor and a ten-turn potentiometer at room temperature form a closed-loop servomechanism that accurately positions the tuners.

V. Optics

The optics are required to illuminate the antenna with good efficiency over the bandwidths of the selected inserts. This is done for both receivers by imaging the primary mirror aperture on to the mouth of a corrugated feedhorn which has a frequency-independent field. The optics for the low- and high-frequency receivers differ and will be described separately. Some components are common, however, and are described below. A detailed description of the various optical components is given in [19].

A. Common Components

1) Polarization Diplexer: The critical component in polarization diplexers is a grid of wires with diameter and spacing small compared to a wavelength. Components of the incident wave with the electric vector parallel to the wires will induce currents in the wires and will be reflected. Orthogonal components will be transmitted unaffected through the grid. Using a single grid to divide a beam into two orthogonal linear polarizations inevitably involves additional reflectors, so making the optics bulky (Fig. 4(a)). Sometimes a rooftop reflector is used to twist the signal transmitted through the grid by 90° and reflect it off the underside of the grid (Fig. 4(b)) [7], but this has the disadvantage of introducing unequal path lengths to the two receivers. Furthermore, one of the plane reflectors needs to be a grid to separate the cross-polar components; otherwise, standing-wave problems occur.

The crossed-grid configuration has the advantage of complete symmetry as shown in Fig. 4(c).

The construction of the crossed-grid is illustrated in Fig. 5. One rectangular grid is fabricated with wires along the length of the grid. Two U-shaped grids are fabricated with wires running across the U. The three grids are assembled in a holder, each U-shaped grid being advanced using a micrometer until the first wire is within about 100 μm of the wires on the rectangular grid. The gap between grids is not critical, and little degradation of the signal reflection was observed for gaps up to almost a wavelength.

The grid for the low-frequency receiver has an aperture of 180 mm and uses 50-μm-diameter wires spaced 140 μm apart. The high-frequency grid has an aperture of 76 mm and uses 25-μm-diameter wire spaced 110 μm apart. Gold-plated tungsten wire is used in all cases.

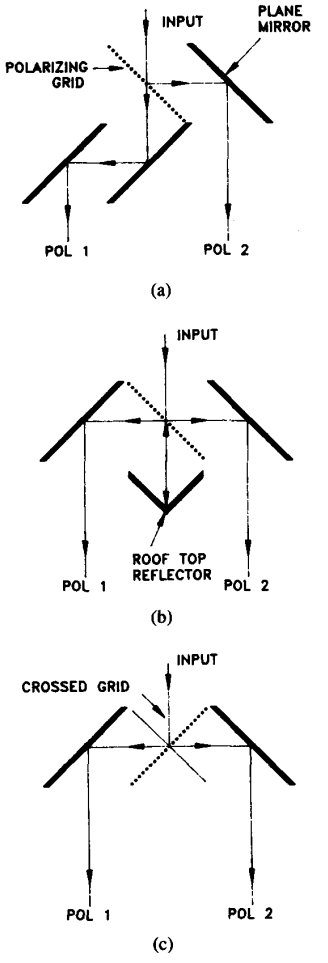

Fig. 4. Polarization diplexer configurations.

2) Vacuum Window: The two receivers use identical 76-mm-diameter vacuum windows to pass the signal beam into the dewar. The low-frequency receiver uses external optics to reduce the beam diameter prior to transmission through the window. The construction of the window is shown in Fig. 6 and is fully described in [20]. A 25-μm-thick plastic film is supported on 25-mm-thick low-density dielectric foam. The foam bears the full atmospheric pressure and also acts as an infrared filter to reduce radiative cooling of the mylar film and radiative loading of the contents of the dewar.

The loss of the window at frequencies up to 300 GHz was measured to be less than 0.2 dB.

3) Infrared Filters: The design and performance of these filters are detailed in [19], [21]. In order to reduce the heat loading on the 4 K station and to keep the temperatures of the cooled receiver components as low as possible, the external IR radiation from room temperature must be blocked. Partial blocking is effected by the foam of the vacuum windows being radiatively cooled on the dewar side, but this is far from sufficient.

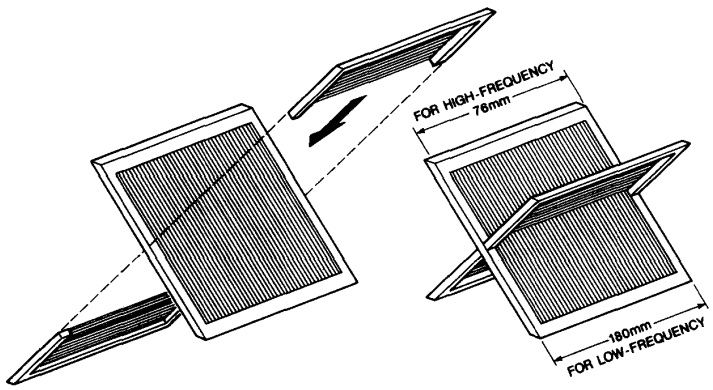

Fig. 5. Construction of the crossed-grid diplexer.

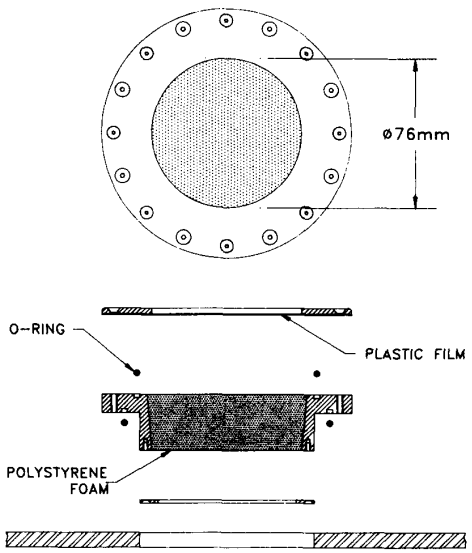

Fig. 6. Construction of the broadband vacuum window.

The material from which the filter is made should have a low dielectric constant and absorption at millimeter wavelengths to minimize reflective and dissipative losses to the signal. In the infrared it should be highly absorptive to minimize transmission of heat. For the material to emit a minimal amount of radiation to the cold station, it should be at a low temperature which implies that the thermal conductivity should be high so that the center of the filter is not warmed significantly by the radiation from the vacuum windows. The filters required for this application are relatively large (76 mm in diameter) so the temperature uniformity is an important issue. PTFE has suitable RF and IR properties, and a 6.3-mm thickness was calculated to yield an acceptable radial temperature gradient. Both faces are matched to the millimeter-wave signal with rectangular grooves.

The heat load on the 4 K stage when using the foam vacuum window and the IR filter was measured at 16 mW. For eight windows, this gives a total load on the 4 K stage of 128 mW.

B. The Low-Frequency Optics

The large size of the telescope secondary focus makes it impractical to focus directly into the dewar. Instead, an offset parabolic reflector is used to focus the beam down to a reasonable size in the dewar as shown in Fig. 2.

The focal ratio of the telescope secondary focus is 13.8 and the beam-waist radius at that point is approximately 10 λ. The focal ratio of the offset parabola is approximately 6. The feedhorn is placed at a distance from the parabola equal to its focal length (635 mm), and the telescope secondary focus is positioned 635 mm towards the subreflector (via the crossed grid). This arrangement corresponds to a Gaussian beam telescope in which the field distribution at the feed horn is frequency-independent [19], [22]. For the beam waist to be at the aperture of the horn, the phase error at the horn aperture should be small. Rather than requiring a long feed to keep the phase errors small, a short, wide-angle horn is used and the large phase error corrected with a dielectric lens.

A feed aperture of 56.5 mm is well matched to the frequency-independent beam waist produced by the offset reflector. A flare angle of 19.8° gives a convenient overall length for the horn. The corrugations are a quarter-wavelength deep with a pitch of one wavelength at the geometrical center of the band except near the throat. At the throat, there is a short, smooth-walled conical section followed by narrower grooves of varying depths. The transition to quarter-wavelength slots is made over about six slots with a resulting reflection coefficient of better than −20 dB over the band.

All the horns were electroformed on aluminum mandrels and gold-plated. The transition from rectangular guide, a simple linear taper, was formed in the same electroform.

Cross-polar response of the feed is terminated by the absorber below the grid and was measured to be − 25 dB at 115 GHz. Total losses in the room temperature optics amount to about 0.13 dB producing about 9 K increase in noise temperature.

C. High-Frequency Optics

A layout of the high-frequency receiver is shown in Fig. 7. Two pairs of inserts cover the frequency range 200–300

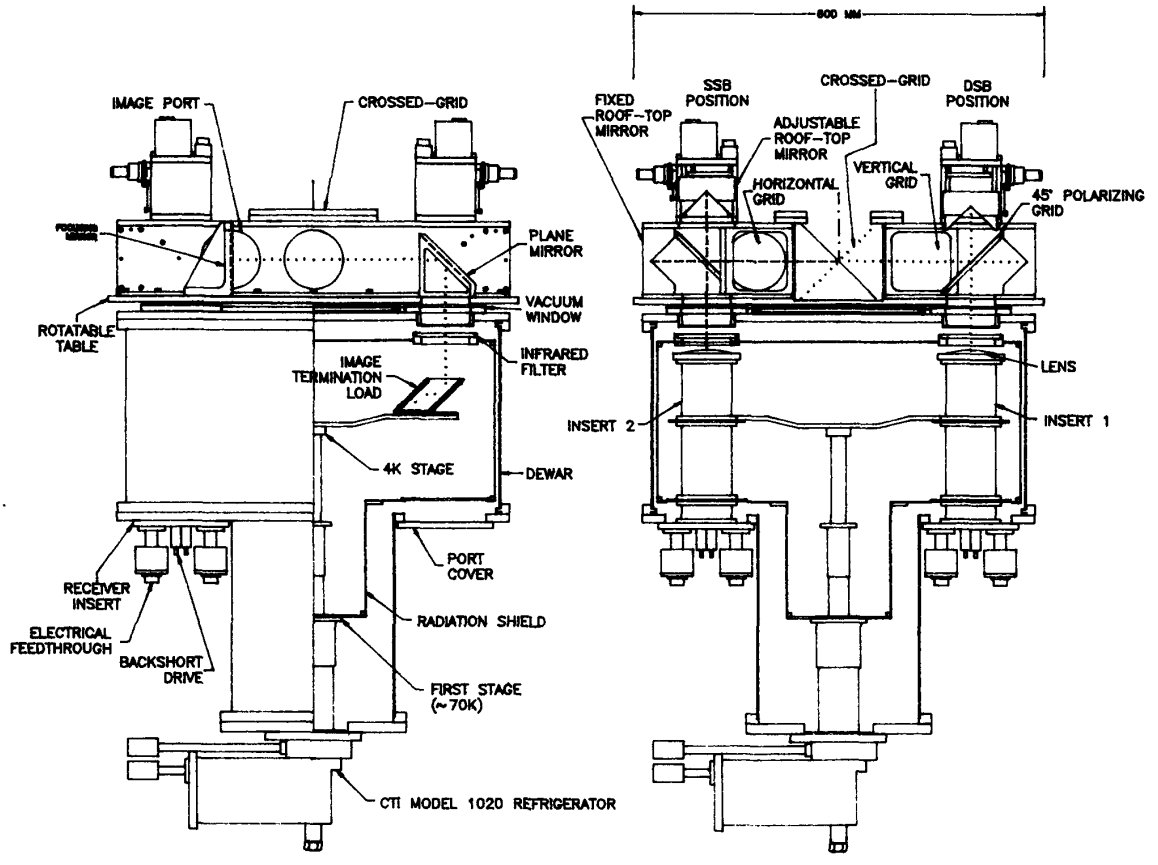

Fig. 7. Layout of the high-frequency receiver.

GHz. The low-frequency inserts are mechanically tuned and cover 200–260 GHz. The high-frequency inserts cover the range 230–300 GHz and are fixed-tuned. It is planned to produce complete coverage of the 200–300-GHz band with a fixed-tuned mixer in the near future. Also contained within the high-frequency dewar are four loads cooled to 4 K for terminating the image frequency for each pair of inserts. Tunable Martin–Puplett interferometers, one for each channel, are used to separate and reject the image band from the signal band for single-sideband operation.

1) The Feed/Lens Combination: For the frequency range 200–300 GHz, the beam-waist radius at the secondary focus (10 λ) varies from 15 to 10 mm. The usual criterion for unblocked transmission of a Gaussian-shaped beam is 4–5 times the beam radius [22] so the 76-mm diameter vacuum windows and infrared filters will pass the beam with no appreciable blockage. Consequently, a lens/feed combination is used with the lens cooled to 4 K, a scaled version of the system described in [23]. The aperture of the lens is 54 mm and the focal ratio 0.7. The feed is a corrugated horn with an aperture of 4.54 mm. The lens is made from PTFE and corrections were made to the lens profile to allow for both dimensional changes and dielectric constant change when cooled to the low operating temperature [19]. The lens is matched on both front and rear surfaces with rectangular matching grooves.

Losses in the optics are similar to those for the low-frequency receiver, with the cross-polar being – 21 dB and the overall optics loss 0.13 dB. Image rejection is >20 dB over 300-MHz bandwidth.

2) The Image Termination Scheme: For clarity, one polarization channel of the image termination scheme is shown in diagrammatic form in Fig. 8 and an isometric view of the actual construction is shown in Fig. 9. At the heart of this scheme is the Martin–Puplett polarizing interferometer, a device that has found universal application in millimeter- and submillimeter-wave systems [24].

In Fig. 8, the input signal is polarized with the E-field perpendicular to the plane of the page and passes through polarizing grid $P1$. The signal beam is then divided into two equal amplitude components by polarizing grid $P2$, the wires being arranged to have a projected angle of 45° to the incident wave (an angle of 35.26° to the plane of the page in Fig. 9). The two resulting waves are each reflected from a rooftop reflector that rotates the plane of polarization by 90°. The two waves combine again at $P2$ with a path-length difference that may be set by adjusting the distance to either of the rooftop mirrors.

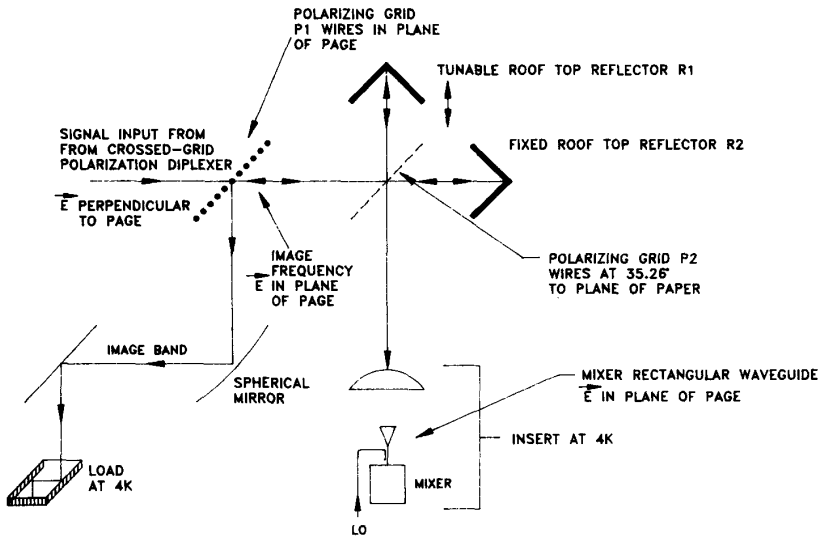

Fig. 8. Image termination scheme.

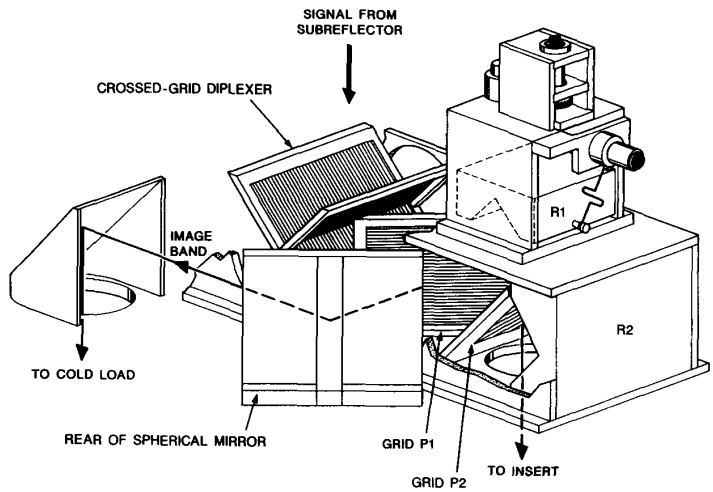

Fig. 9. Isometric view of image termination components.

There are two path-length differences that are of interest in this application. The first is a path-length difference of zero. In this case, all the signal power (both sidebands) is transmitted to the mixer. This is used for continuum observations that are concerned with the measurement of the total amount of power emitted over a given bandwidth; examples are measurements of the brightness temperature of planets or of interstellar dust clouds, and the determination of spectra of objects such as quasars over several octaves [15]. The second position of interest is when the path length difference is set coarsely to be $\lambda_{IF}/4$ and then finely tuned so that the path-length difference is an even number of half-wavelengths for the signal frequency and an odd number for the image frequency. In this case, it can be shown that the signal and image frequency bands, as "seen" by the mixer, are cross-polarized at grid $P1$ [22]. The signal frequency band is coupled to the telescope optics and the image band is coupled to the cold load via the spherical mirror and 45° plane mirror. Eccosorb MF114 iron-loaded epoxy (Emerson and Cuming, Inc.) is used as the absorber material for the cryogenic image termination. By extrapolation of the manufacturer's data, the dielectric constant was estimated to be 9.3 and the absorption coefficient 8.5 cm^{-1}. Reflection measurements from a slab of the material were in reasonable agreement with the dielectric coefficient. Measurement of the thermal conductivity at ~15 K indicated a value of 1.9 ± 0.2 mW · cm^{-1} · K^{-1}.

Three slabs are arranged as illustrated in Fig. 8. Each load is oriented so that the receiver polarization is parallel to the plane of incidence. Ideally, the incidence angle should be the Brewster angle (72°), but a sufficiently small reflection is obtained at 45° which is more convenient geometrically. Each slab is 3 mm thick which is thick

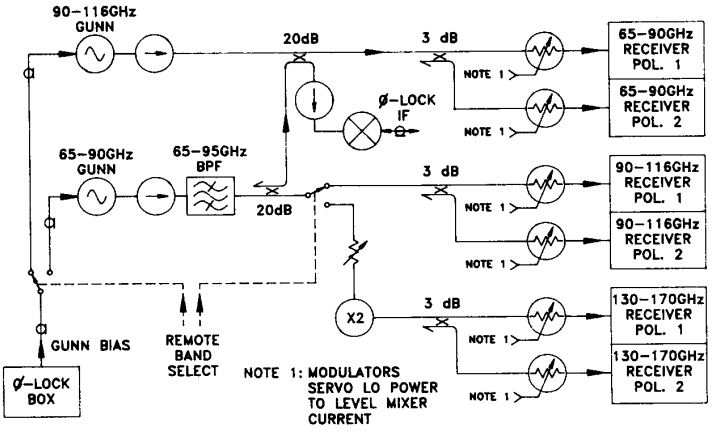

Fig. 10. Local oscillator arrangement.

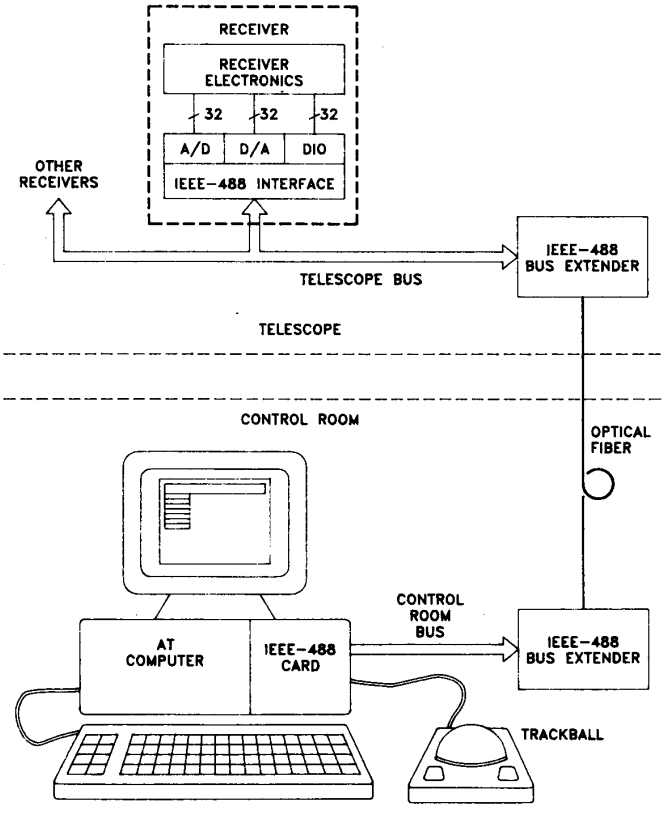

Fig. 11. Receiver control system.

enough to ensure high absorption and thin enough to have a negligible thermal gradient. They are mounted on copper plates with screws and vacuum grease.

An incident wave undergoes five reflections which correspond to a theoretical return loss of − 35 dB. Measurement of the reflection coefficient at room temperature yielded an upper limit of − 25 dB. Although the physical temperature of the load is 4 K, the inevitable losses in the vacuum window and infrared filter raise its apparent temperature, as measured outside the dewar, to around 27 K.

VI. Local Oscillator

One Gunn oscillator [25], phase-locked to the telescope frequency standard, is used for each mixer pair. For the 65–90-GHz and 90–116-GHz bands, the Gunn output is

split and each polarization insert is supplied with LO power via a ferrite modulator which levels the LO power in a servo loop to keep the mixer current constant (Fig. 10). In the 130–170-GHz band, the Gunn output is frequency-doubled and split between the two polarizations. Individual ferrite modulators are used for each polarization insert. Since modulators are not available in the 200–300-GHz band, the Gunn output is first split for the two polarizations and controlled by the modulators before being multiplied by a tripler in each polarization. For this band, overmoded waveguide carries the signal into the directional coupler.

VII. Operation of Receivers

A. Receiver Tuning

For optimum performance, the receiver noise temperature should be minimized and, for spectral line observations, the image sideband suppressed by at least 15 dB. A chopper with absorbing vanes gives a signal against cold sky which is used to indicate noise temperature while tuning. The sideband tuning of the low-frequency receiver is optimized by moving a small servo-controlled mirror into the beam of the receiver and reflecting into the receiver the output of a harmonic generator with the harmonics spaced by nominally 3 GHz (twice the IF). The response of the receiver in both sidebands may then be monitored by observing the IF output on a spectrum analyzer and the tuning optimized to minimize the response at the image frequency and simultaneously maximize the response at the signal frequency.

B. Receiver Control

All mechanical tuning adjustments are provided with dc servomechanisms. Control and monitoring of bias voltages, tuning adjustments, temperatures, etc., are done through a data link communicating on an IEEE-488 bus (Fig. 11). The bus is linked to a personal computer in the control room via a fiber-optic link. The computer may display any one of a number of screens appropriate to the task at hand. All adjustments may be made manually through the computer. Previous tuning positions for a particular frequency may be stored and recalled for fast retuning. Fully automatic tuning procedures are being developed.

VIII. Cryogenics

The two receivers use the same design of dewar fabricated from stainless steel. The dewar is 600 mm in diameter, 200 mm deep, and has an extension cylinder on the bottom to hold the refrigerator.

A commercially available, two-stage refrigerator, a CTi Model 1020, provides the first two stages of cooling for a Joule–Thompson (J-T) refrigerator. A block diagram of the refrigerator is shown in Fig. 12.

The receiver electronics within the dewar are completely enclosed by a nickel-plated copper radiation shield attached to the first stage of the refrigerator, operating at around 70 K. Five layers of super-insulation between the radiation shield and the dewar wall serve to reduce the radiation load

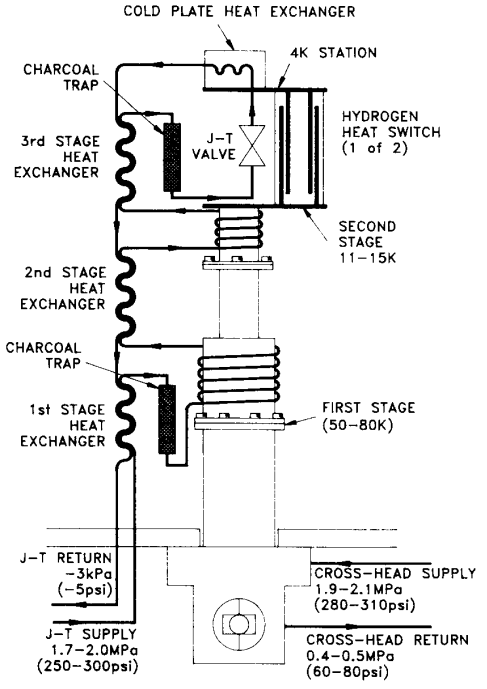

Fig. 12. Block diagram of 4 K refrigerator.

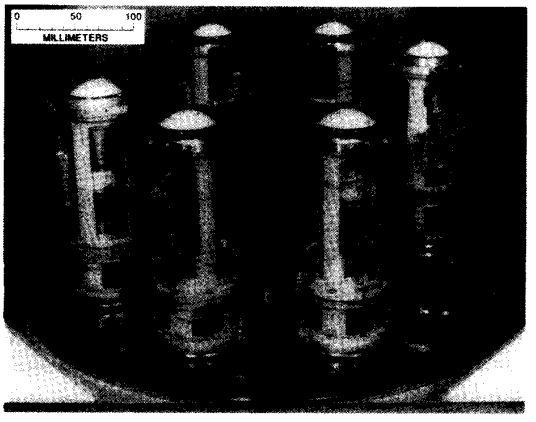

Fig. 13. Photograph of inserts in dewar (main vessel and radiation shields removed.)

on the first stage of the refrigerator. The main loads on the first stage are the radiation load from the infrared filters and the load from the precooling of the helium gas for the Joule–Thompson expansion valve.

The J-T refrigerator is separately supplied with high-purity helium gas at a pressure of 2 MPa (300 psi). The incoming gas is cooled by the outgoing gas in the first-stage heat exchanger and further cooled in copper tube wound on a form that is attached to the first stage. After further cooling as shown in Fig. 12, the helium expands and liquifies through a J-T valve consisting of a hypodermic needle with a wire inserted to restrict the flow to 3.2

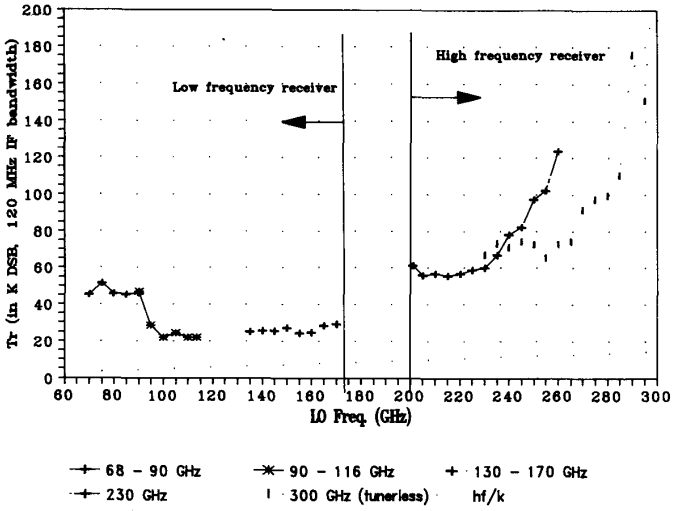

Fig. 14. Noise temperature of best receiver inserts.

standard liters per second. Initial cooling is assisted by a hydrogen-filled heat switch which conducts heat from the third stage to the second stage until the hydrogen condenses and ceases to conduct at around 10 K.

With minimal loading on the refrigerator, a thermal load of up to 1.6 W may be applied before the third stage cannot hold the temperature close to 4 K. The capacity is a function of the temperatures (and, therefore, loading) of the first and second stages. It was found to be important not to load the second stage (running at around 12 K) other than with the gas being supplied to the J-T valve or the capacity of the J-T third stage is diminished. For this reason, it was actually preferable to have the HFET amplifiers, which dissipate about 40 mW each, on the third stage, rather than the second.

The loading on the three stages of the refrigerator was estimated as follows. On the first stage, there is a loading of about 15 W from the radiation on the shield and the load from the gas in the J-T circuit. A further load of about 0.5 W is expected for each window and 0.3 W in conduction from the G-10 supports, waveguide, coaxial cable, and backshort drives for each insert. Only the gas in the J-T loop loads the second stage, contributing about 3 W. For the third stage, conduction losses to the first stage dominate, giving a load of about 100 mW per insert. Each HFET dissipates 40 mW, and the radiation load from the window is around 16 mW. In operation with the helium return line running at around − 3 kPa (− 5 psi), the third-stage temperature runs at approximately 3.5 K and the mixers at 4 K.

Long-term stability of the third-stage temperature is typically better than ±50 mK over a timescale of a day. On shorter timescales of minutes, temperature fluctuations are less than ±2 mK. This temperature stability is due to the presence of liquid helium in a reservoir close to the J-T valve.

Systems employing J-T valves in the past have developed a reputation for being unreliable. Our experience, after three years of operation, has been quite the opposite. We attribute this increase in reliability to several changes. The first is the use of a separate helium circuit for the J-T system. This has the effect of eliminating any possible contamination from the main refrigerator. Previous systems have used a common circuit for the helium gas. Another significant change is the replacement of reciprocating compressors with new units using the so-called "scroll" principle in which a rotor in the form of a scroll rotates within a similarly shaped stator. The design is such that the entering gas is trapped within a space that decreases in volume as the rotor rotates. Oil circulating around the device provides a seal and cooling. This compressor has the advantage of no contacting seals and is also without valves.

One high-capacity scroll compressor is used to drive two 1020 refrigerators and two scroll compressors in series are used to supply two J-T valves. In this way, two receivers are maintained at below 4 K.

A photograph of six inserts installed in the dewar with radiation shields and dewar cylinder removed is shown in Fig. 13.

IX. Receiver Performance

The receiver performance is illustrated in Figs. 14 and 15. In Figure 14, the points plotted are the double sideband noise temperature of the best receiver inserts we have constructed. We anticipate improvements in the 68–90 GHz frequency range due to future improvements in the SIS mixers. The lower noise temperature data points in the range 130–170 GHz are results obtained with a new 2-mm mixer [26], but these have yet to be installed on the telescope. The rise in noise temperature above 280 GHz is inherent in the present mixer design, and work is progressing on a new mixer design. Figure 15 shows the measured single-sideband noise temperatures of the complete receiver in the laboratory. These are the results

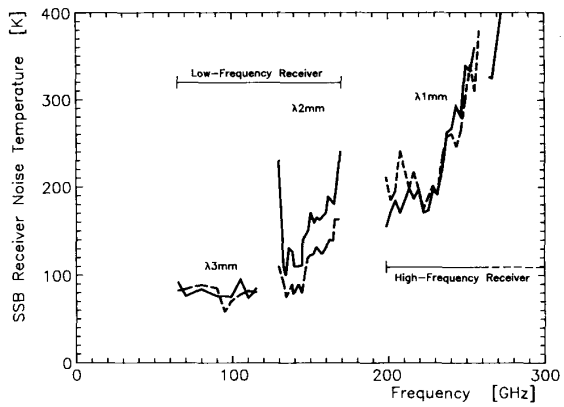

Fig. 15. Measured SSB receiver noise temperature.

Component	Loss (dB)	Physical Temp. (K)	Noise Temp. (K)	Contribution To Receiver Noise Temp. (K)
Vacuum Window	0.07	300	4.9	4.9
Infrared Filter	0.05	70	0.81	0.82
Lens/Horn	0.25	5	0.30	0.31
Coupler	0.05	5	3.0*	3.3
Mixer	3.0	4.2	6.0	6.6
Isolator	0.2	5	0.24	0.52
IF Amplifier	–	5	1.2	2.8
TOTALS	3.62			19.3

*Noise from 300K via Coupler

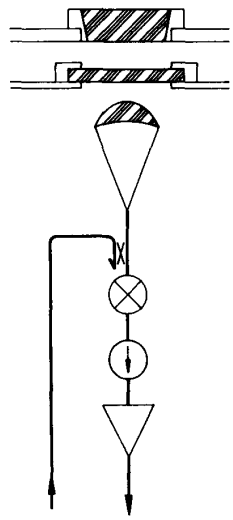

Fig. 16. Double-sideband noise contributions at 100 GHz.

obtained when the receiver is tuned up for single-sideband operation with >20 dB image rejection.

The best noise temperature we have measured at 100 GHz is 19.1 K double-sideband, and it is instructive to tabulate the various estimated contributions to this final measured temperature as shown in Fig. 16. One major contributor to the final noise temperature is the room-temperature window, and it is difficult to see how this can be reduced appreciably.

When used in radio astronomy for spectral line observations, it is crucial that the final output of the receiving system, the output of the spectrometer, be flat with frequency or exhibit "good baselines" as this is commonly referred to in radio astronomy circles. This requires great

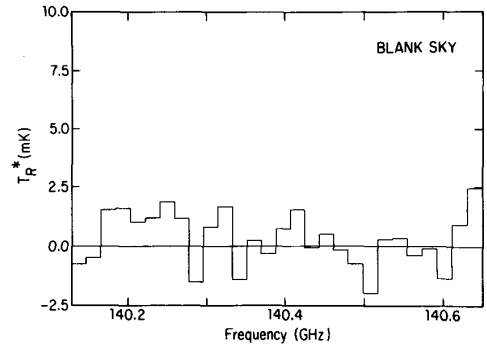

Fig. 17. Receiver baselines—result of 8-h integration.

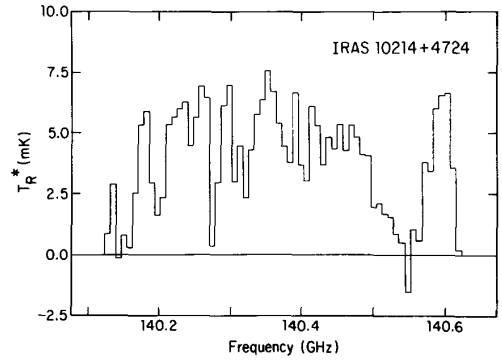

Fig. 18. Detection of a carbon monoxide spectral line emission.

stability in the passband of the entire system. Fig. 17 illustrates the good performance of these new receivers in this regard [27]. This figure shows the output of the spectrometer for an integration period of 8 h on blank sky. It may be seen that the output is flat to better than 1 mK of antenna temperature or around three parts per million of system temperature. Figure 18 shows the detection of a 7 mK spectral line emission. The rest frequency of the emission from this object is 461 GHz, carbon monoxide (4–3 transition). The received frequency is 140 GHz, the shift being the result of the red shift associated with the expansion of the universe. The broad nature of the spectral emission is the result of clumps of gas within the object moving at different velocities. Such detections obviously require excellent baseline stability from the receivers and associated instrumentation.

X. Conclusion

This new generation of SIS receivers provides complete coverage of the 68–300-GHz atmospheric windows with good performance. The use of closed-cycle 4 K refrigerators makes helium replenishment unnecessary. Fast, simple switching between frequency bands is now possible. The receivers give excellent performance as regards noise temperature and stability.

In the future, it will be possible to include all frequency bands including the 300–360-GHz band in one dewar. This

receiver will be a prototype for the proposed millimeter-wave array [28].

ACKNOWLEDGMENT

The construction of these receivers was a joint effort among three NRAO sites: Tucson, AZ; Green Bank, WV; and Charlottesville, VA. The success of the receivers is due, in large part, to the efforts of J. Fitzner in constructing the J-T refrigerator, compressors and LO circuits; G. Taylor, A. Marshall, and M. Hedrick for machining the insert parts and dewar; D. Dillon for machining the refrigerator parts; V. Summers for plating and electroforming; D. Boyd for assembly of the inserts; A. Perfetto and E. Kemp for design and construction of the electronics; and J. Kingsley for much of the mechanical design.

REFERENCES

[1] J. R. Tucker, "Quantum-limited detection in tunnel junction mixers," *IEEE J. Quantum Electron.*, vol. QE-15, pp. 1234–1258, Nov. 1979.

[2] J. R. Tucker and M. J. Feldman, "Quantum detection at millimeter wavelengths," *Rev. Mod. Phys.*, vol. 57, no. 4, pp. 1055–1113, Oct. 1985.

[3] A. R. Kerr and S.-K. Pan, "Some recent developments in the design of SIS mixers," *Int. J. Infrared and Millimeter-Waves*, vol. 11, no. 10, 1990.

[4] A. W. Lichtenberger, D. M. Lea, R. J. Mattauch, and F. L. Lloyd, "Nb/Al–Al_2O_3/Nb junctions with inductive tuning elements for a very low-noise 205-250 GHz heterodyne receiver," *IEEE Trans. Microwave Theory Tech.*, vol. 40, no. 5, pp. 816–819, May 1992.

[5] S.-K. Pan, M. J. Feldman, A. R. Kerr, and P. Timbie, "Low-noise 115-GHz receiver using superconducting tunnel junctions," *Appl. Phys. Lett.*, vol. 43, no. 8, pp. 786–788, Oct. 15, 1983.

[6] A. R. Kerr, S.-K. Pan, and M. J. Feldman, "Integrated tuning elements for SIS mixers," *Int. J. Infrared Millimeter Waves*, vol. 9, no. 2, pp. 203–212, Feb. 1988.

[7] J. W. Archer, "High-performance, 2.5 K cryostat incorporating a 100-120 GHz dual polarization receiver," *Rev. Sci. Instrum.*, vol. 56, no. 3, pp. 449–458, Mar. 1985.

[8] D. P. Woody, R. E. Miller, and M. J. Wengler, "85-115 GHz receivers for radio astronomy," *IEEE Trans. Microwave Theory Tech.*, vol. MTT-33, no. 2, pp. 90–95, Feb. 1985.

[9] S. R. Davies, L. T. Little, and C. T. Cunningham, "Low-noise SIS heterodyne receiver at 230 GHz," *Electron. Lett.*, vol. 23, no. 18, pp. 946–948, Aug. 1987.

[10] J. Ibruegger, M. Carter, and R. Blundell, "A low-noise broadband 125-175 GHz SIS receiver for radio astronomy observations," *Int. J. Infrared and Millimeter Waves*, vol. 8, no. 6, pp. 595–607, June 1987.

[11] B. N. Ellison and R. E. Miller, "A low-noise 230 GHz SIS receiver," *Int. J. Infrared and Millimeter Waves*, vol. 8, no. 6, pp. 609–625, June 1987.

[12] H. Ogawa, A. Mizuno, M. Moko, H. Ishikawa, and Y. Fukui, "A 110 GHz SIS receiver for radio astronomy," *Int. J. Infrared and Millimeter Waves*, vol. 11, no. 6, pp. 717–726, June 1990.

[13] J. W. Kooi, M. Chan, T. G. Phillips, B. Bumble, and H. G. LeDuc, "A low-noise 230 GHz heterodyne receiver employing .25 μm^2 area Nb/AlO_x/Nb tunnel junctions," *IEEE Trans. Microwave Theory Tech.*, vol. 40, no. 5, pp. 812–815, May 1992.

[14] S. R. Davies, C. T. Cunningham, L. T. Little, and D. N. Matheson, "A 210-280 GHz SIS heterodyne receiver for the James Clerk Maxwell Telescope. Part I: Design and performance," *Int. J. Infrared and Millimeter Waves*, vol. 12, no. 5, pp. 647–658, May 1992.

[15] J. M. Payne, "Millimeter and submillimeter wavelength radio astronomy," *Proc. IEEE*, vol. 77, no. 7, July 1989.

[16] J. M. Payne, "A switching subreflector for millimeter-wave radio astronomy," *Rev. Sci. Instrum.*, vol. 47, pp. 222–223, 1976.

[17] P. R. Jewell and J. W. Lamb, private communication.

[18] J. D. Gallego and M. W. Pospieszalski, "Design and performance of a cryogenically-coolable, ultra low-noise, L-band amplifier," in *Proc. 20th European Microwave Conf.* (Budapest, Hungary, Sept. 1990), pp. 1755–1760.

[19] J. W. Lamb, "Optics for cryogenic millimeter-wave receivers," in preparation.

[20] A. R. Kerr, N. Bailey, D. E. Boyd, and N. Horner, "A study of materials for a broadband millimeter-wave quasi-optical vacuum window," NRAO Electronics Div. Internal Rep. 292, Aug. 1992.

[21] J. W. Lamb, "Infrared filters for cryogenic millimeter wave receivers," *Int. J. Infrared and Millimeter Waves*, vol. 14, no. 5, May 1993.

[22] P. F. Goldsmith, "Quasi-optical techniques at millimeter and submillimeter wavelengths," in *Infrared and Millimeter Waves*, vol. 6, K. J. Button, Ed. New York: Academic Press, 1982, pp. 277–343.

[23] B. L. Ulich, "Optimized cassegrain feed system," Tucson Operations Internal Rep. 6, National Radio Astronomy Observatory, Mar. 1980.

[24] D. H. Martin, "Polarizing (Martin-Puplett) interferometric spectrometers for the near and submillimeter spectra," in *Infrared and Millimeter Waves*, vol. 6,. K. J. Button, Ed. New York: Academic Press, 1982, pp. 65–148.

[25] J. E. Carlstrom, R. L. Plambeck, and D. D. Thornton, "A continuously tunable 65–115 GHz Gunn oscillator," *IEEE Trans. Microwave Theory Tech.*, vol. MTT-33, pp. 610–619, 1985.

[26] A. R. Kerr, S.-K. Pan, A. W. Lichtenberger, and F. L. Lloyd, "A new SIS mixer for the 2-mm band," in *Proc.4th Int. Symp. on Space Terahertz Technology*, Mar. 1993.

[27] R. L. Brown and P. A. Vanden Bout, *Astrophys. J. (Lett.)*, 1993, in press.

[28] R. L. Brown, in *Radio Interferometry: Theory, Techniques and Applications*,T. J. Cornwell and R. A. Perley, Eds. San Francisco, CA: Astron. Soc. of the Pacific, 1991, p. 410.

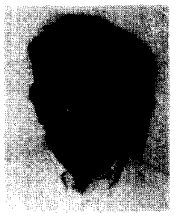

John M. Payne was born in England in 1939. He received the B.Sc. degree in electrical engineering from the University of London in 1962.

He has been with the National Radio Astronomy Observatory since 1967 and since 1974 has been responsible for millimeter-wave instrumentation for the 12-m telescope at Kitt Peak, AZ. Since 1989 he has also been responsible for the development of the active surface for the Green Bank Telescope.

Mr. Payne is a member of the International Union of Radio Science and a Fellow of the IEE.

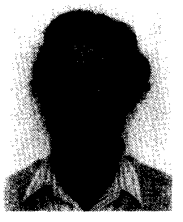

James W. Lamb was born in Aberdeen, Scotland. He received the B.Sc. (hons) degree in physics from the University of Canterbury, New Zealand, and the Ph.D. degree in natural philosophy from Aberdeen University, Scotland.

After a year at the Helsinki University of Technology (Finland), working on cooled receivers, he spent two yers at Queen Mary College, London, on the electromagnetic design of the James Clark Maxwell Telescope. Since then he has been with the National Radio Astronomy Observatory (NRAO), Tucson, AZ, constructing and maintaining SIS-mixer receivers for the 12-m telescope. He is also in charge of the proposed millimeter array antennas design. His other interests include cryogenic receivers, quasi-optics, antenna design, and 4 K systems.

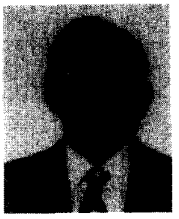

Jackie G. Cochran was born in Buckhannon, WV, in August 1940.

He began his career with the National Radio Astronomy Observatory (NRAO) in Green Bank, WV, in February 1965. Shortly thereafter, he moved to Chrlottesville, VA, to join the Central Development Laboratory effort to develop cryogenically cooled receivers for use in radio astronomy. Since January 1974, he has continued his work on the 4 K cryogenic system and millimeter-wave receivers for the use of NRAO's 12-m telescope located on Kitt Peak, near Tucson, AZ.

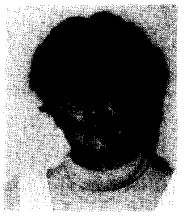

Nancyjane Bailey (Member, IEEE) was born in Boston, MA, in 1957. She received the B.A. degree in communication studies in 1979 and the B.S. degree in electrical engineering in 1982 from the University of Massachusetts at Amherst. She is presently pursuing the M.S.E.E. degree at the University of Virginia, Charlottesville.

From 1982 to 1987, she worked for Alpha Industries, developing millimeter-wave switches, mixers, and subsystems. She joined the National Radio Astronomy Observatory's Central Development Laboratory on 1987, where she works to provide Schottky-diode multipliers and receiver inserts for the 12-m telescope at Kitt Peak, AZ.

Ms. Bailey is a Senior Life Member of the Society of Women Engineers and is currently serving as the Region E Member-at-Large Representative to the Council of Section Representatives. An IEEE member since 1981, she served as the Secretary/Treasurer of the Central Virginia Section during 1992–1993, and is a candidate for the Vice Chair of the section for 1993–1994.